A STUDY OF THE EFFECTS OF MATERIAL TYPE AND CONFIGURATION ON OPTICAL CROSS SECTION

Kelly Feirstine
J.D. Yarbrough
James Rosprim
Schafer Corporation
Advanced Concepts and Technology Division; Space Systems Group
2309 Renard Place SE, Suite 300, Albuquerque, NM 87106

Dr. Leslie Vaughn
Geoffrey Jenkins
Dr. Michael Duggin
Air Force Research Laboratory
Space Vehicles Directorate
3550 Aberdeen Avenue SE, Kirtland AFB, NM 87117

ABSTRACT

An experiment was designed to study the effects of material type and configuration on Optical Cross Section (OCS) and spectrum. The experiment was conducted at an Air Force Research Laboratory (AFRL) far-field imaging facility, using different diffuse and specular materials and various configurations and/or combinations of each. It was hypothesized that the OCS of certain combinations of materials is dependent on the diffuseness or specularity of the materials used, but the spectrum is independent of these factors and does not change. The objective of the experiment is to capture both OCS and spectra of different material configurations using different combinations of diffuse and specular materials in the bistatic illumination condition. OCS was calculated relative to the scattering of a Spectralon material that was in the scene during all data collects. Results show the accuracy of the above hypothesis and other effects that material type and configuration have on OCS and spectra.

Keywords: optical cross section, far-field imaging, far-field distance, Spectralon

1 INTRODUCTION

There are many objects (both man-made and naturally occurring) orbiting the Earth, ranging in size from small debris that could pose a potential hazard to other objects to larger satellites and objects such as the International Space Station. It is important to understand and characterize the optical signatures of each of these types of space objects for Space Situational Awareness (SSA), or the ability to understand and comprehend the elements in the space environment. This optical signature information aids in the understanding of the space environment as a whole. In order to understand these optical signatures, a means to accurately measure, model, and simulate the space objects is necessary.

The space objects described above are unresolved images; therefore one cannot use imagery to determine its makeup. But the capability to determine and understand the optical signatures of single material objects such as space debris is critical in SSA. If the material and size are known, material properties such

as Bidirectional Reflectivity Distribution Function (BRDF) can be measured, a model of the object can be manufactured and characterized in a far-field optical measurement facility to determine the Optical Cross Section (OCS), and the optical signature can be modeled with a code such as Time-domain Analysis Simulation for Advanced Tracking (TASAT), a legacy Air Force Research Laboratory (AFRL) satellite simulation code used throughout the satellite modeling community. The appropriate radiometry can be simulated and the space debris characterized and understood optically. However, this task is more difficult for larger objects or objects composed of more than one material. In order to characterize the optical signatures of larger objects, the above described methodology is not sufficient in that it is not be feasible to manufacture a model of such a large object (because of material, time, acceptable program risk, or monetary restrictions) nor characterize it in the same far-field optical measurement facility due to facility limitations. A proposed solution to this problem is to manufacture a scale model of the space object. This type of scale model building is not unique to space objects; scale model building enables the same type of testing with air (wind tunnel testing) and water (fluid dynamics testing) vehicles as well. For example, testing a scale model of a water vehicle may include a simple scaled version of the vehicle, but the testing may be performed in a more viscous substance such as oil instead of water.

Scale model building of space objects has many benefits. These models allow the ability to acquire optical signature data (as described above) on a satellite that may be too large to characterize full-scale in a far-field optical measurement facility. However, in order to accurately characterize the scale models and identify their optical signatures, the materials used on the model must remain optically accurate when scaled. If a methodology to optically scale space materials accurately or replace the space material with a similar material that is optically representative of the actual space material was developed, this would be a cost effective way to investigate the optical signatures of satellites that may have already launched or that are too large to characterize in a far-field optical measurement facility.

The first step in developing a methodology to build optically accurate scale models is to determine the effect material type and configuration have on the overall OCS of the known object. Take a solar panel for instance; a solar panel may be composed of several tens or hundreds of solar cells. To create a quarter scale model of the panel, does each individual solar cell need to be scaled in size as well, or is it optically sufficient to simply scale the size of the whole panel and use a smaller number of full-sized solar cells? This is the type of critical of question that this material type and configuration experiment will try to answer.

2 DATA COLLECTION METHODOLOGY AND DATA PROCESSING

Multispectral optical measurements of space objects can be acquired at an AFRL far-field optical measurement facility. The imaging facility allows the collection of accurately simulated observations of space objects without significant atmospheric effects. Having the ability to do this provides the opportunity to measure the optical signatures of satellites for which it is feasible to relocate to the facility. For those satellites and objects for which this is not feasible, it is likely that building a scale model would be sufficient to gain the necessary optical signature information. The data collected in the optical measurement facility is accurate passive far-field imagery, OCS, and spectra helpful in understanding optical space object signatures.

$$D_{obs} = \frac{L}{\theta_S} \qquad (1)$$

$D_{obs} =$ Observing distance
$L =$ Length of the largest smooth surface on the space object
$\theta_S =$ Angular diameter of the illumination source

The use of the term far-field intensity distribution or passive OCS in this paper is analogous to the reflective pattern of a distant object in solar illumination. This definition is based on a discussion of radiant intensity as related to a source as discussed in Reference [1]. In short, when the observing distance is larger than $\frac{L}{\theta_S}$ where θ_S is the angular diameter of the sun and L is a characteristic length of the largest smooth surface on the space object, the reflected spatial intensity pattern is circular [1]. This distance (D_{obs}) is called the far-field. Any distance less than D_{obs} is considered the near-field where the reflected spatial intensity pattern is not circular.

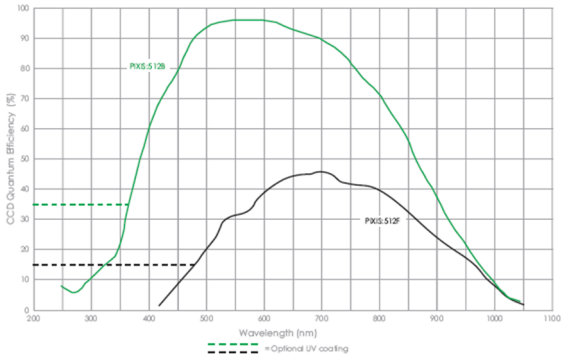

Figure 1: Quantum efficiency of the PIXIS camera, as provided by the manufacturer

Now to discuss the scientific equipment used at the far-field optical measurement facility as well as the measurement and analysis approach. A digital scientific imaging camera called the PIXIS provides 16-bit data from 400nm − 900nm. The Quantum Efficiency (QE) of the camera is shown in Figure 1. Filtered waveband images can be acquired at several different bandwidths with filters that span the QE range of the PIXIS. The filters are narrow band filters. The spectral transmission of these filters is shown in Figure 2(a). The filter chosen for use in the first data collects of this experiment was the 650nm filter. The quantum efficiency of the PIXIS camera peaks in this waveband.

There are two additional astronomy filters that can be used as well, V-band and I-band filters. The spectral transmission of these two filters is shown in Figure 2(b). In addition to the scientific imaging camera, an Analytical Spectral Devices spectroradiometer (ASD) can be used during the data collects as well. The ASD provides continuous spectral information from 350nm − 2500nm in one nanometer increments. A 6-Degree of Freedom (DOF) robotic arm at the optical facility can be used to articulate the models\materials to be measured. The robotic arm can manipulate a payload of up to 200kg and has a repeatable accuracy within +/ − 0.5 mm.

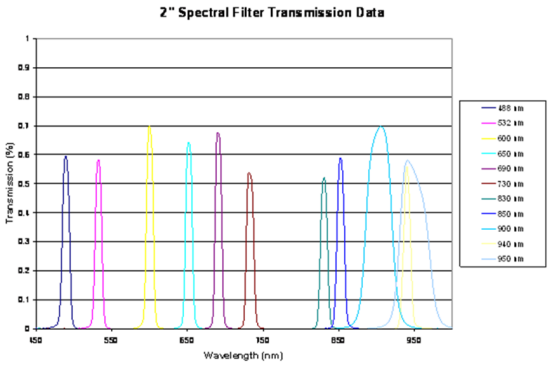

(a) Laser line spectral filter transmission

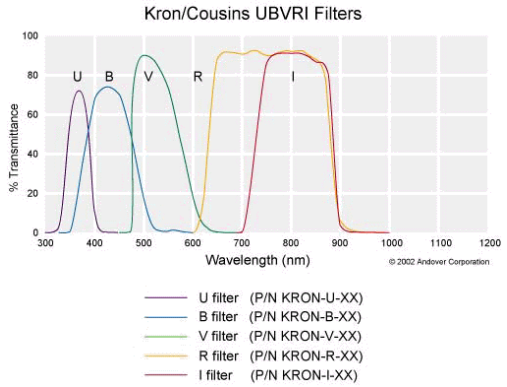

(b) Kron/Cousins V- and I-band spectral filter transmission

Figure 2: Spectral filter transmissions for the different filters at the far-field imaging facility

The measurement approach relies on the fact that a couple of requirements are met. First, the test object must be in the far-field as described by Equation 1 above. When the object is imaged in the far-field, accurate optical signatures can be measured. Second, accurate far-field measurements rely on a reference material in the scene with the object at all times. Atmospheric variations and absorption lines that would become troublesome in the analysis fall out of the measurement when images can be normalized to a known reference imaged under the same lighting conditions. Solar passive test object surface radiance can vary largely, so a reference material that exhibits the same brightness independent of illumination and surface orientation is ideal. The reference should also be spectrally flat over the entire measurement wavelength range. Spectralon is a good diffuse reference for these types of measurements, though it has a limited

range of acceptance angles and exhibits enhanced backscatter in a monostatic geometry. The backscatter is not a concern in this experiment as the only geometry used is a bistatic geometry with a 90° Solar Phase Angle (SPA), as depicted in Figure 3. This is a typical measurement of space objects from the ground.

Once the reference is chosen, it is imaged in the scene with the test object at all times. The test object data is normalized to this reference and the result is scaled to OCS which is in units of $[m^2]$. The Spectralon surface brightness with units of $\left[\frac{W}{m^2\ sr\ \mu m}\right]$ is related to the irradiance with units of $\left[\frac{W}{m^2\ \mu m}\right]$ by a factor of $\frac{1}{\pi}$. Normalizing by the irradiance minimizes the atmospheric effects and could remove lens Field of View (FOV) and vignetting effects, as well as mitigate issues with non-uniform illumination of the object. This way, the far-field imagery, spectrum, and any simulation data can be compared directly.

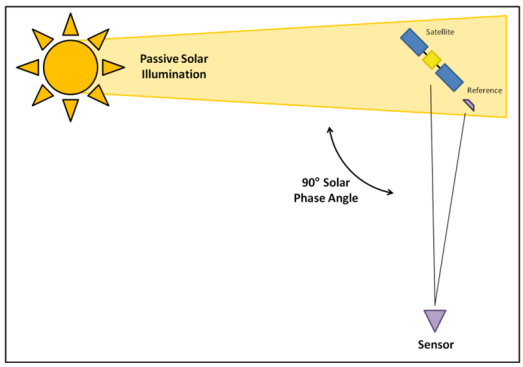

Figure 3: Bistatic illumination geometry for the far-field optical measurement facility

3 EXPERIMENT TEST PLAN

The results of this experiment will help to answer the question of how material type and configuration affect the far-field OCS. Does the far-field OCS of certain materials scale with surface area? It is hypothesized that the OCS is dependent on the diffuseness or specularity of the materials used, but the spectrum of the object is independent and does not change. The rest of this section will outline the test plan for this experiment, imaging geometry and the materials that were chosen for data collection, and the reasoning behind those choices.

There are two primary objectives that this experiment will address. The first primary objective is to determine whether or not OCS scales linearly with object surface area. That is, if the object surface area is scaled down by half, will the OCS also scale down by half, or will the OCS scale factor be different than the surface area scale factor? Secondary goals of this main objective are to determine what the OCS scale factor is relative to the surface area scale factor, and if the OCS scale factor is the same for both glint and off-glint geometries. Once the OCS scale factor is determined, the second primary objective is to determine whether or not a change in material configuration has an effect on OCS. That is, if two materials are used, each covering 50% of the test object, does the configuration or placement of those two materials affect the OCS?

The test object is a 16" x 16" x $\frac{1}{4}$" flat plate of aluminum 6061 to which different materials are mounted. Aluminum 6061 was chosen as the base of the experimental test object because it is the most commonly used material in satellite bus structures. The aluminum 6061 is also readily available and the machining of it is affordable. To simulate different solar cell configurations mounted to a satellite bus, a thin specular material was mounted to the plate in various configurations. The specular material is an opaque white vinyl film with a low tack adhesive backing. This material was selected for its availability, affordable pricing, ease of application and removal. This material's low tack adhesive mitigates many of the chemical, mechanical, and residual risks to the test object associated with other adhesive materials.

The test object was imaged over a limited set of pose angles (or rotations) including both glint and off-glint geometries. The rotations were made about the fixed X, Y, and Z axes of the far-field optical measurement facility. Both the origin of the fixed facility axes and the object's center of rotation are the same point. That is, the object's center of rotation never changes throughout the experiment. The poses used were 0°, 30°,

45°, and 60° rotations about each of the fixed axes for a total of 64 permutations. The glint geometries here are a 0° rotation in X, any rotation in Y, and a 45° rotation in Z.

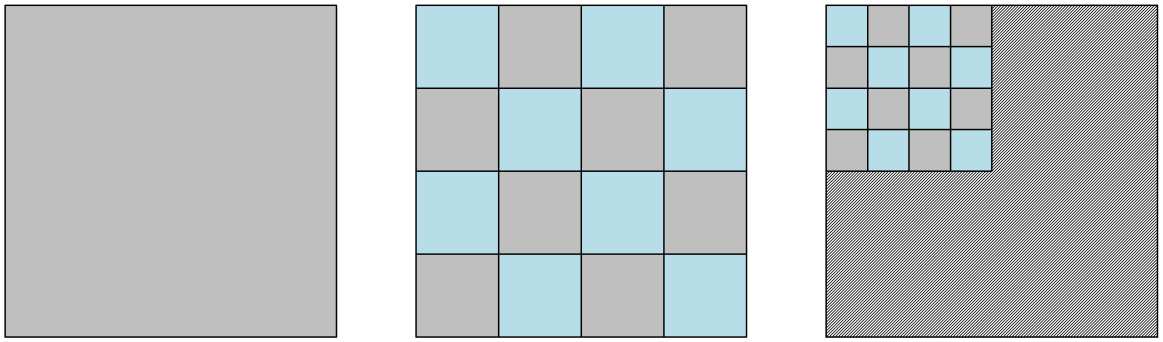

(a) Pattern 1

(b) Pattern 2

(c) Pattern 3

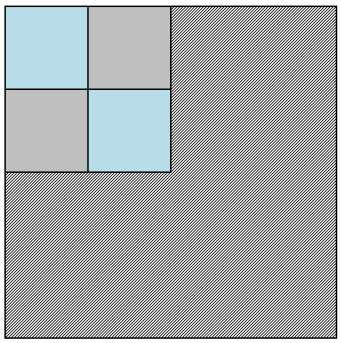

(d) Pattern 4

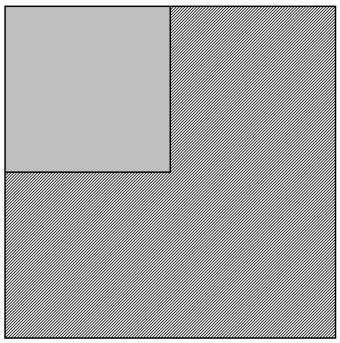

(e) Pattern 5

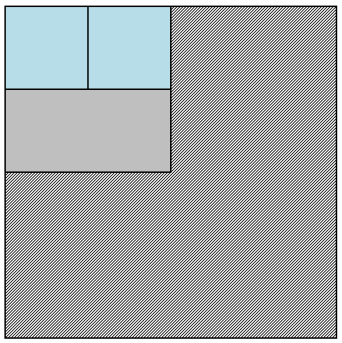

(f) Pattern 6

Figure 4: Test object material configurations

In order to accomplish the objectives of this experiment, it was necessary to develop some simple patterns that could be applied to the test object for data collection. The six different material configurations are shown in Figure 4. These patterns were created by applying the white specular material to the test object. The first pattern, Figure 4(a) is the full scale (1:1) single material pattern using aluminum 6061, and Figure 4(b) is a scaled down version (1:4) of that pattern. The figure also shows four patterns with different configurations using 50% aluminum 6061 (represented by the grey color) and 50% white specular material (represented by the blue color). Figure 4(c) is the full scale version of the 50\50 material configuration.

The pattern chosen for this experiment is a checkerboard using 4"x 4"squares of each material in the full scale version. Figure 4(d) is the same checkerboard pattern only shown in quarter scale. That is, the surface area of the entire panel is scaled by a quarter (8"x 8") and the checkerboard squares are also scaled down to 2"x 2"in size. Patterns 5 and 6, Figures 4(e) and 4(f) respectively, are similar to the scaled checkerboard in that the material configuration is still 50% aluminum 6061 and 50% white specular material. However, the pattern deviated from the actual scaled version of the checkerboard. Figure 4(e) uses the full-sized squares (4"x 4") but only 2 of them arranged in a larger checkerboard pattern while Figure 4(f) also used 2 full-sized squares but arranged them beside one another. Again, all three of the quarter scale patterns remain 50\50 material contribution, but the pattern is different. The comparison of the OCS from these three configurations will indicate whether or not OCS is dependent on pattern and surface area or only on surface area. This will determine if it is necessary for components such as solar cells to be scaled with the model or if full-size components can be used on a scaled down model as long as the surface area remains the same.

4 FAR-FIELD IMAGING RESULTS

Recall that the test plan states that the OCS of the bare aluminum 6061 panel at full scale size (16"x 16") will be compared to the 1:4 scale size (8"x 8") bare aluminum panel in order to determine whether or not the OCS scales with surface area scaling. The two patterns used for this initial comparison are shown in Figures 4(a) and 4(e), respectively. Two comparison plots of the OCS in a glint position and 3 off-glint positions are shown in Figure 5. It seems that, by inspection of the two graphs, the OCS does not scale with surface area linearly for all positions. That is, as the entire surface area decreases as in a scale model, the OCS does not decrease by that same scale factor. In this case, the area scale factor is 4.

In Figure 5(a), the scale factor in the glint position ($-45°$ rotation in Z) is approximately 4, and in the glint position of Figure 5(b) the scale factor is approximately 4.11. This difference could be attributed to the surface finish of the aluminum. The aluminum is milled in a vertical direction so as it rotates, the milling pattern changes direction. However, the scale factors in an off-glint position ($-30°$ rotation in Z) for these two figures respectively, are approximately 2.75 and 3. It seems that the OCS does not scale similarly for both glint and off-glint positions.

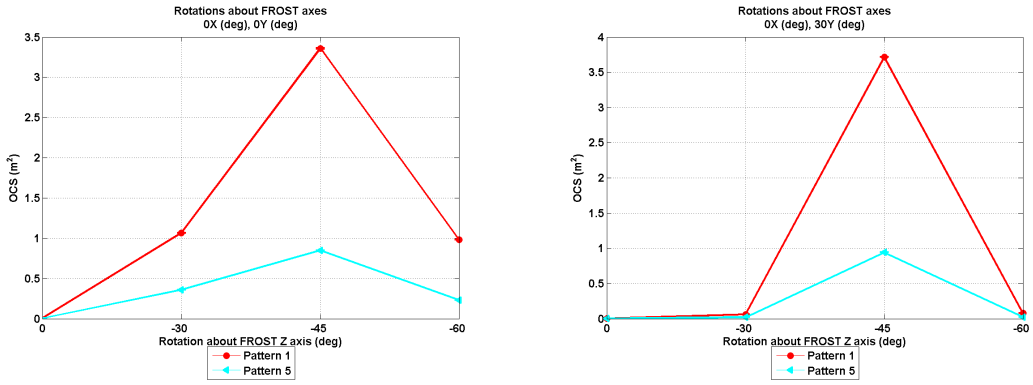

(a) OCS comparison 1

(b) OCS comparison 2

Figure 5: OCS comparison plots between the single material full scale pattern and a quarter scale pattern

Data was also collected for the patterns shown in Figures 4(b) and 4(c). Comparing the full scale data to the quarter scale version also does not yield any definitive results, as can be seen in Figure 6. The scale factors for the glint positions here are approximately 5.45 and 6. This comparison clearly shows that the OCS scale factor is still not 4 for all positions. However, there is not enough information here to determine what relationship the area scale factor and the OCS scale factor do have. Additional research and data collection is necessary to answer this question.

Another comparison was made using the OCS calculated from patterns 3, 4, and 6 (Figures 4(c), 4(d), and 4(f)). Each of these three configurations contains 2 materials and each material occupies 50% of the whole panel. Note that the lined section of the shape is blacked out and doesn't contribute to the final OCS calculation. Results show that the configuration of material, whether components (think solar cells) are laid out in a checkerboard pattern, side-by-side on the top half of a panel only, or randomly placed over the whole panel, does not make a difference in the OCS calculation as long as the ratio of material contribution is the same. Plots of these results are shown in Figure 7 and each of the three curves fall directly on top of one another. This indicates that material configuration or size does not affect the OCS. This result may indicate that OCS is not the metric to use for pose determination of solar panels or other similar satellite components on-orbit as attitude (material configuration or orientation in this case) cannot be determined from this experimental data.

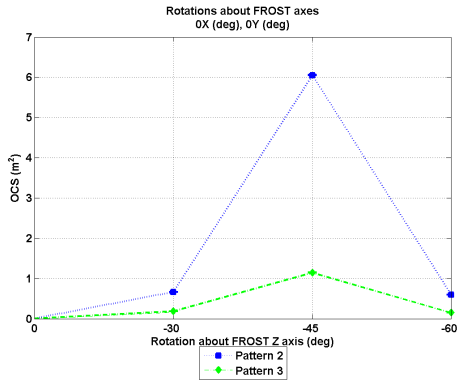

(a) OCS comparison 1

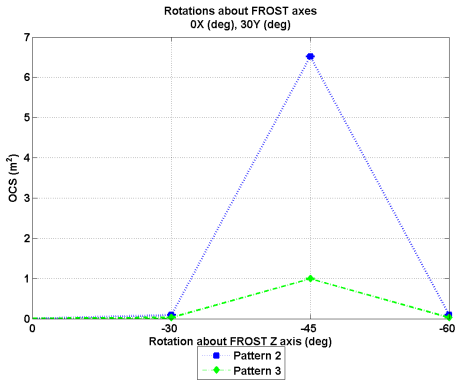

(b) OCS comparison 2

Figure 6: OCS comparison plots between the 2 material full scale pattern and a quarter scale pattern

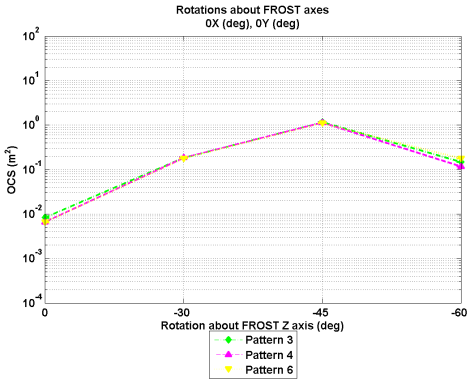

(a) OCS comparison 1

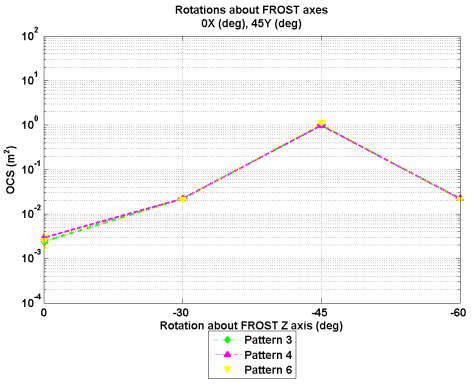

(b) OCS comparison 2

Figure 7: OCS comparison plots between three quarter scale patterns with the same material area

5 CONCLUSIONS AND PATH FORWARD

As time was an issue, spectral data in each configuration was not able to be collected. Recall that it was hypothesized that the spectrum would be independent of configuration while the OCS would not. As this experiment progresses, an analysis of the spectrum of each configuration will be performed to determine if indeed the spectrum is independent of material configuration, as the preliminary OCS results indicate. In future experiments, additional wavebands can be used with the PIXIS camera, additional materials can be tested as well as additional configurations of the materials. This experiment was a simple 50\50 contribution of two materials, aluminum 6061 and a white specular material. Additional poses can also be collected as well to fill in the gaps between the glint and off-glint data points as necessary.

Overall, this was a first step towards determining the most affordable, simple way to build optically accurate scale satellite models that can be optically characterized in an AFRL far-field imaging facility. Understanding optical signatures of space objects is critical in SSA efforts going forward, and the ability to understand the signatures of large objects is huge for space object imaging. The results of this experiment start to build a methodology that should be employed to manufacture optically accurate scale models used in pre-launch characterization efforts of space objects in support of SSA efforts.

6 REFERENCES

[1] L. Mandel and E. Wolf, *Optical Coherence and Quantum Optics*, s.l.: Cambridge University Press, 1995.

[2] King, L., Hohnstadt, P., and Feirstine, K., Pre-launch Optical Characteristics of the Oculus-ASR Nanosatellite for Attitude and Shape Recognition Experiments. AIAA/Utah State University Small Satellite Conference; 2011 August; Utah State University, Utah.